

# Uniaxial Orientation of Linear Low Density Polyethylene

JOSE L. PEZZUTTI\* and ROGER S. PORTER, *Materials Research Laboratory, Polymer Science and Engineering Department, University of Massachusetts, Amherst, Massachusetts 01003*

## Synopsis

Only a few reported studies have involved the uniaxial orientation of LDPE and even less on LLDPE. It is our purpose to report on characteristics of uniaxially oriented films of LLDPE that contribute to property development. The LLDPE has been coextruded at 25 and at 80°C layered as ribbons within longitudinally split billets of HDPE. The LLDPE so drawn was characterized by thermal analysis, birefringence, elastic recovery, and wide angle X-ray measurements. As a result, we can conclude that the drawing of LLDPE at the lower temperature produces a relatively high content of monoclinic crystals; the orientation behavior of LLDPE is similar to that of HDPE. The molecular network formed by entanglements and crystals reduces the draw to a maximum below 15.

## INTRODUCTION

With developments in the polymerization of ethylene, a novel class of linear low density polyethylene (LLDPE) is now in competition with conventional low density polyethylene (LDPE), the worlds largest volume thermoplastic. LLDPE is mainly processed by film blowing and by blow molding, frequently drawn down to thicknesses below 10  $\mu\text{m}$  and with the development of excellent tensile and impact strength. These processes involve stretching of LLDPE at different temperatures from above to well below the melting point to induce molecular and crystal orientation.<sup>1,2</sup>

In recent years there have been many studies on the relationship between deformation, morphology, and the consequent properties of oriented polymers. In particular, ultraoriented HDPE fibers with tensile moduli > 200 GPa and draw ratios > 200.<sup>3</sup> On the other hand, only a few studies<sup>4,5</sup> have involved the uniaxial orientation of LDPE and even less on LLDPE. Of course, conventional processing of thermoplastics often results in molecular orientation.

It is the purpose of this communication to report on the draw and the characteristics of uniaxially oriented films of LLDPE. The LLDPE has been coextruded within split billets of HDPE. The ribbons of LLDPE so drawn were characterized by thermal analysis, birefringence, elastic recovery, and wide angle X-ray. Results are thus provided on draw efficiency (from elastic recovery), the fraction of crystals (thermal and X-ray analysis), and the relative orientation of the amorphous and crystalline phases (X-ray

\* On leave from Planta Piloto de Ingenieria Quimica, UNS-CONICET, Bahia Blanca, Argentina.

and birefringence), which are responsible for the mechanical properties of the uniaxially oriented LLDPE.

## EXPERIMENTAL

### Polymers and Preparations

The two polyethylenes used in this study are detailed in Table I. Isotropic sheets of about 0.3 mm thickness were obtained by compression molding at 160°C and subsequently quenched into water to room temperature. These sheets were cut and placed between longitudinally split cylindrical billets of HDPE. This assembly was then coextruded at 25 and at 80°C through conical brass dies of included entrance angle of 20°. The extrusion draw ratio (EDR) was calculated from the displacement of lateral ink marks placed on the ribbon prior to extrusion. Multistage coextrusions<sup>6</sup> were used in some cases to avoid excessive high pressures leading to buckling in a single pass.

### Thermal Analysis

The melting point and heat of fusion were determined by a Perkin-Elmer differential scanning calorimeter (DSC-2) calibrated with the melt transition of indium and naphthalene. All measurements were made at a heating rate of 10°C/min. The melting point was defined as the maximum peak value of the fusion curve and from an average of three runs. The crystalline weight fraction ( $X_c$ ) was determined from the relationship between the endothermic areas and the heat of fusion for a perfect polyethylene crystal having the orthorhombic unit cell ( $\Delta H^0 = 69 \text{ cal/g}$ ).<sup>7</sup> With no easy alternative, the heat of fusion for polyethylene of the monoclinic form was assumed equal to that of the orthorhombic.

### Birefringence

The birefringence was measured using an Ehringhaus Caclspar compensator with a Zeiss polarizing microscope and a white light source (5500 Å

TABLE I  
Characteristics of Polyethylenes Tested

Type	Composition	$M_n^a$	$\rho^b$ (g/cm <sup>3</sup> )	$T_{ex}^c$ (°C)	EDR <sub>max</sub> <sup>d</sup>
LLDPE	Ethylene-butene-1	35,000	0.918	25	8
				80	9
HDPE	Homopolymer	33,000	0.960	25	> 15

<sup>a</sup> From MI.

<sup>b</sup> As provided by supplier.

<sup>c</sup> Extrusion draw temperature.

<sup>d</sup> Maximum extrusion draw ratio maximum in this study.

wavelength). The total birefringence  $\Delta n_T$  was calculated from

$$\Delta n_T = \frac{R}{d} \cdot \lambda$$

where  $\lambda$  is the wavelength,  $R$  the retardation, and  $d$  the sample thickness.

### Wide Angle X-Ray

Orientation of the  $a$ ,  $b$ , and  $c$  crystal axes for draw ratios lower than 4 were measured by azimuthal scanning of the (110) and (200) reflection, using a Siemen D-500 diffractometer operating at 30 mA and 40 kV.  $\text{Cu}\alpha$  radiation with Ni-filter is used, and subsequent interpretation from the Wilchinsky formula.<sup>8</sup> The samples extruded at  $\text{EDR} > 4$  had a strong (002) reflection so that a direct determination of the  $C$ -axis crystal orientation could be made. It had been shown at high orientation<sup>9</sup> that this gave the same results as the Wilchinsky's method. The orientation functions were evaluated according to

$$f_a = (3 \overline{\cos^2 \phi_a} - 1)/2$$

$$f_b = (3 \overline{\cos^2 \phi_b} - 1)/2$$

$$f_c = (3 \overline{\cos^2 \phi_c} - 1)/2$$

where  $\phi_{a,b, \text{ or } c}$  is the angle between the unit cell axes and the draw direction. Orientation function is 0 for random,  $-0.5$  for perpendicular, and 1 for perfect orientation. For an orthorhombic system, they are related by

$$f_a + f_b + f_c = 0$$

### Amorphous Orientation

Amorphous orientation  $f_{\text{am}}$ , was estimated from a combination of birefringence and X-ray data using the equation proposed by Stein<sup>10</sup>

$$\Delta n_T = \Delta n_c X_c + \Delta n_{\text{am}}(1 - X_c) + \Delta n_d + \Delta n_f$$

where  $\Delta n_c = \Delta n_c^\circ f_c$  is the birefringence of the crystalline phase and  $\Delta n_{\text{am}} = \Delta n_{\text{am}}^\circ f_{\text{am}}$ , is the birefringence of the amorphous phase. The birefringence  $X_c$  used is volume fraction, whereas a determination from DSC gives weight fraction. A density correction is therefore needed. The form ( $\Delta n_f$ ) and distortion ( $\Delta n_d$ ) birefringence were also neglected. The intrinsic birefringence of the crystalline and amorphous phases used were  $\Delta n_c^\circ = 0.057$  and  $\Delta n_{\text{am}}^\circ = 0.043$ .<sup>10</sup>

### Elastic Recovery

The drawn ribbons were cut into 1 cm length and immersed in a silicone oil bath maintained at 160°C. The ribbons, on heating, become simultaneously molten, transparent, and shrunk. The shrunk film was removed from

the bath, cooled, and measured. The total elastic recovery was calculated from the following expression:

$$R (\%) = \frac{L_T - L}{L_T - L_0} \times 100$$

where  $L_T$  is the length of the drawn specimens,  $L$  is the shrunk length, and  $L_0$  the length before deformation ( $L_0 = \text{EDR} \times L_T$ ).<sup>11</sup>

## RESULTS

The melting point ( $T_m$ ) of LLDPE obtained by DSC is insensitive to draw ratio and draw temperature ( $T_{ex}$ ). They are all within 1°C for all EDR and for the two extrusion draw temperatures, 25 and 80°C. The percent crystallinity increases by 7.5% at EDR 8 and is higher at equivalent draw ratio when extruded at the higher temperature (see Fig. 1).

Figure 2 shows the total birefringence as a function of EDR at both extrusion draw temperatures.  $\Delta n_T$  increases rapidly with initial draw, followed by an approach to a limit at higher EDR. There is a small dependence of  $\Delta n_T$  on extrusion temperature, being lower at the higher  $T_{ex}$ . The coextruded HDPE samples were more generally birefringent.

The wide-angle X-ray flat film of undrawn LLDPE shows a diffraction pattern of uniform concentric rings. Upon extrusion draw at 25°C, a strong monoclinic reflection with  $d$ -spacing = 4.56 Å ( $2\theta = 19.4^\circ$ ) was detected in LLDPE for an EDR as low as 1.6. Other weak reflections were also observed at  $2\theta$  of 23° and 24.9°. According to the unit cell dimensions of monoclinic PE, these reflections correspond to the (001), (200), and (201) planes respectively.<sup>12</sup> The (001) reflection shows off-equatorial maxima in both HDPE

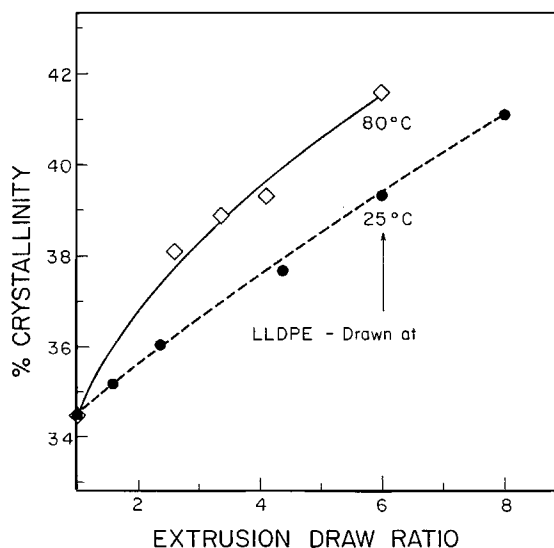


Fig. 1. Percent crystallinity vs. extrusion draw ratio for LLDPE drawn at 25 and 80°C. Data obtained with DSC-2 at 10°C/min.

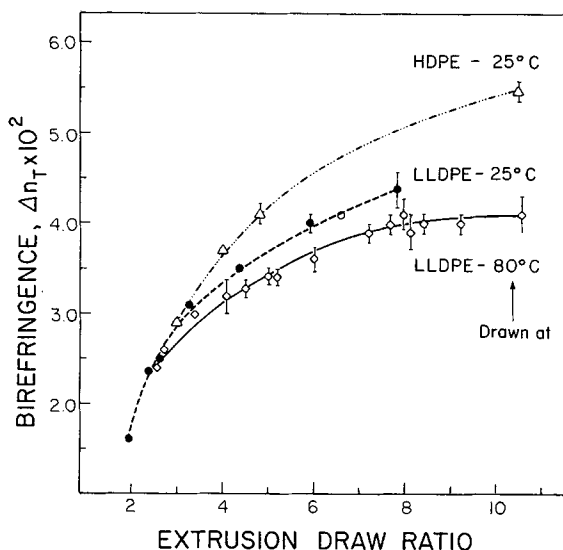


Fig. 2. Total birefringence vs. extrusion draw ratio for LLDPE drawn at 25 and 80°C and for HDPE drawn at 25°C.

and LLDPE for an EDR between 2 and 4 and turn to the equator at yet higher EDR. The LLDPE drawn at 80°C shows only a weak reflection for monoclinic at a  $19.4^\circ 2\theta$  angle.

The  $a$ ,  $b$ , and  $c$  crystal axis orientation functions of LLDPE drawn at both temperatures are plotted in Figures 3 and 4. As shown, the crystals drawn at 80°C more readily orient to a higher degree approaching the limit of maximum orientation ( $f_a = f_b = -0.5$ ,  $f_c = 1$ ). Furthermore, the alignment of the  $a$  and  $b$  crystal axes are nearly perpendicular to the draw direction

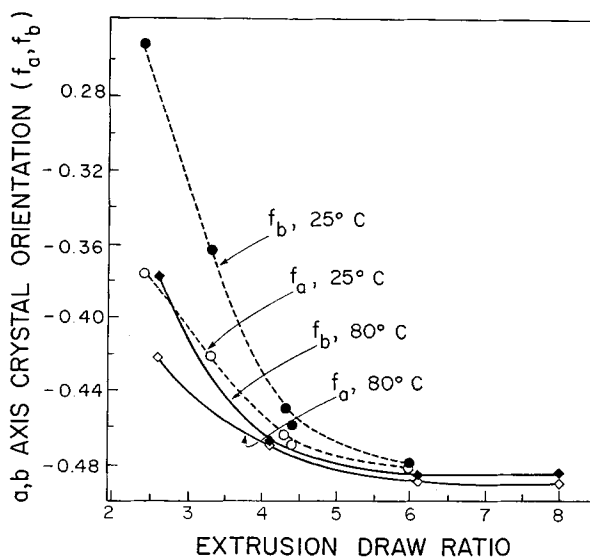


Fig. 3.  $a, b$ -Axis crystal orientation functions vs. extrusion draw ratio for LLDPE drawn at 25 and 80°C.

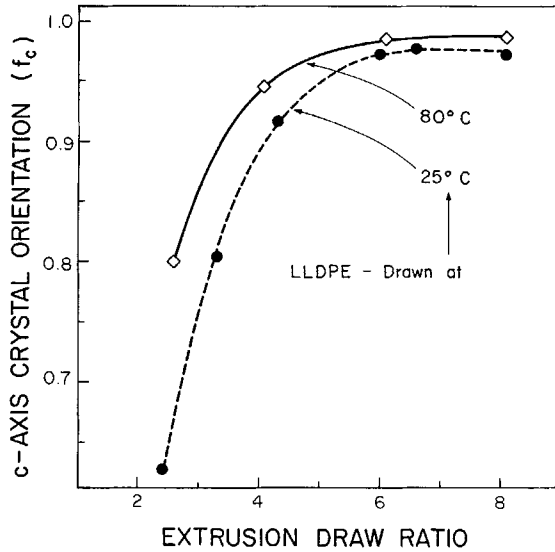


Fig. 4. c-Axis crystal orientation function vs. extrusion draw ratio for LLDPE drawn at 25 and 80°C.

at high EDR. However, at low EDR the crystal  $a$ -axis orients faster than the  $b$  at both extrusion temperatures.

Orientation of the amorphous phase was determined by assuming an additivity of the birefringence contributions for the crystalline and the amorphous phase, and using the crystallinity from DSC plus the  $f_c$  obtained by X-ray (see Fig. 5). The decreased amorphous orientation with increased draw temperature may be noted.

Elastic recovery of the drawn LLDPE is plotted in Figure 6. The recovery

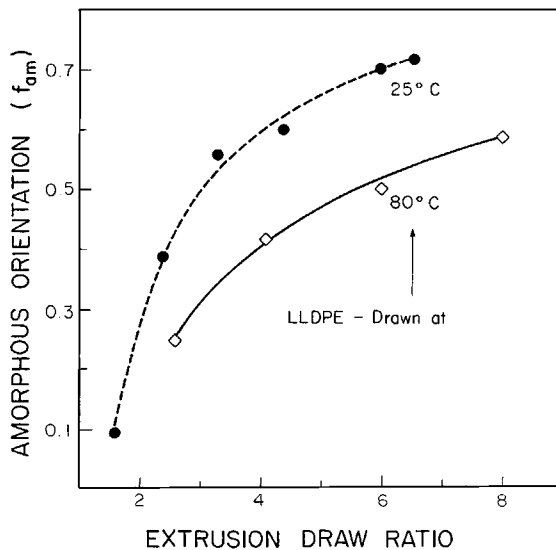


Fig. 5. Amorphous orientation function vs. extrusion draw ratio for LLDPE drawn at 25 and 80°C.

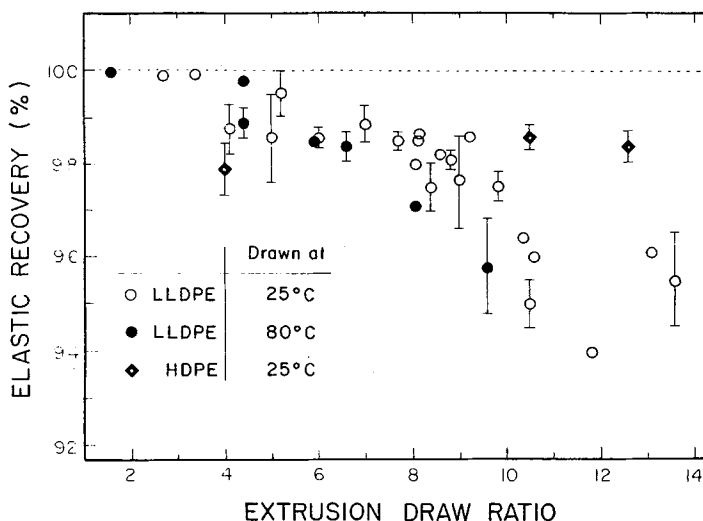


Fig. 6. Percent elastic recovery vs. extrusion draw ratio for LLDPE drawn at 25 (○) and 80°C (●) and for HDPE drawn at 25°C (◇).

was rapid for LLDPE samples after only 15 s at 160°C. At EDR < 4, recovery is ~ 100%. This means that the deformation was virtually affine. At higher draw, recovery decreases with increasing draw, but is still high, 95% at EDR 14. The HDPE of similar molecular weight showed similar behavior. However, the recovery was less. In any case, the behavior of all polyethylenes was comparable, i.e., a high fractional recovery of the original draw indicating the high draw efficiency.

## DISCUSSION

An X-ray diffractometer scan shows strong reflection for monoclinic crystals in LLDPE drawn at 25°C. The monoclinic content, calculated from the equatorial intensity ratio ( $I_{001}^{\text{mon}}/I_{110}^{\text{orth}}$ ), was 20% of the total crystals. At higher EDR the fraction was nearly constant. This value is about half again more than for HDPE drawn at the same condition.

The samples drawn at 80°C showed only a very weak monoclinic reflection. Nonetheless, it has not escaped us that the monoclinic form may be the route to achieve high draw that inevitably involves chain translation through crystals.

The calculated fraction of monoclinic structure is only an estimation due to overlapping reflections from the amorphous halo at a 19.5° 2θ angle. However, it is interesting to note the high content of this structure in drawn LLDPE with less than 40% crystallinity. The monoclinic phase has a lower density, 0.988 g/cm<sup>3</sup>, than the orthorhombic phase by ≲ 2% and was reported to make a significant contribution to the density decreases found in LDPE drawn at low temperatures.<sup>5</sup> However, at higher draw temperatures,<sup>13</sup> because of the much smaller monoclinic content developed, its effect on a density decrease is minimal.

The transformation of the parent spherulitic structure into fibrils on draw results in an increase in orientation for both the crystalline and amorphous

phases. Consequently, the molecules in this latter phase become taut and are closer packed. This has been demonstrated by the increases in tensile modulus with draw, and it is associated with the increase in crystallinity shown in Figure 1. Where the extrusion temperature is sufficiently high to permit the rapid relaxation of the amorphous taut tie molecules, we expect less chain orientation and an annealing effect that increases the crystallinity a little more (see Fig. 1). Indeed, the increase in mobility with temperature led to rotation and unfolding of chain blocks in the lamellae with drawing, given high crystalline orientation (Fig. 3 and 4).

The birefringence is the difference in refractive indices along and perpendicular to the draw direction and increases with the orientation (Fig. 2). The samples drawn at 80°C show slightly lower values. Considering that the initial LLDPE is ~ 60% amorphous, the relaxation of amorphous chains at higher draw temperature consequently has a large effect on the measured total birefringence. Figure 5 shows at higher draw temperature of 80°C,  $f_{am}$  developed on drawing is slow and at EDR 6, is only 0.5 comparing to a value of 0.7 for the same sample drawn at 25°C to equivalent EDR. The lower  $f_{am}$  is due to the faster relaxation of the amorphous chains at higher draw temperature and therefore a smaller contribution resulting in lower total birefringence.

Deformation of a molecular network using a Takayanagi type of model with the network parallel to the crystalline phase has been proposed to explain the drawing behavior of polyethylenes.<sup>14,15</sup> This network is formed by physical entanglements of molecular chains. In an affine deformation, the network is deformed but not destroyed. The crystalline phase maintains the deformed network fixed in entropically unfavorable configuration. When the crystals melt, these amorphous molecules shrink back and the sample adopts the original size and geometry. In the case of LLDPE the recovery was very fast and ~ 100% at <EDR 4 indicating a near affine deformation. At higher draw, % recovery decreases but is still very high, > 43%. The departure from near affine deformation at higher draw is due to morphological changes.

In the semicrystalline LLDPE, at larger deformation, there is a development of fibrillar morphology and simultaneous destruction of the spherulites. This is accompanied by an increase in % crystallinity. The development of new fibrillar morphology is at the expense of the molecular networks and results in greater departure from affine deformation.

## CONCLUSIONS

1. The drawing of LLDPE at 25°C produces a relatively high content of monoclinic phase, estimated to be 20% of the total crystals.
2. The trends in orientation with uniaxial draw for both crystalline and amorphous phases of LLDPE are similar to that of HDPE.<sup>16</sup>
3. A molecular network formed by entanglements and crystals reduced the maximum achievable in a single draw to a ratio below 15.



## References

1. K. Choi, J. E. Spruiell, and J. L. White, *J. Polym. Sci., Polym. Phys. Ed.*, **20**, 27 (1982).
2. W. F. Maddams and J. E. Preedy, *J. Appl. Polym. Sci.*, **22**, 2751 (1978).
3. T. Kanamoto, A. Tsuruta, K. Tanaka, M. Takeda, and R. S. Porter, *Rep. Prog. Polym. Phys., Jpn.*, **26**, 347 (1983).
4. G. Capaccio and I. M. Ward, *J. Polym. Sci., Polym. Phys. Ed.*, **22**, 475 (1984).
5. C. Benelhadjsaid and R. S. Porter, *J. Appl. Polym. Sci.*, **30**, 741 (1985).
6. B. Appelt and R. S. Porter, *J. Macromol. Sci., Phys.*, **B20**, 21 (1981).
7. J. H. Southern and R. S. Porter, *J. Appl. Polym. Sci.*, **14**, 2305 (1970).
8. Z. W. Wilchinsky, *J. Polym. Sci.*, **A-6**, 281 (1969).
9. C. R. Desper, J. H. Southern, R. D. Ulrich, and R. S. Porter, *J. Appl. Phys.*, **41**, 4284 (1970).
10. R. S. Stein, *J. Polym. Sci.*, **31**, 327 (1958).
11. R. S. Porter, M. Daniels, M. Watts, J. Pereira, S. DeTeresa, and A. Zachariades, *J. Mater. Sci., Lett.*, **16**, 1134 (1981).
12. T. Seto, T. Hara, and K. Tanaka, *J. Appl. Phys., Jpn.*, **7**, 31 (1968).
13. H. H. Chuah, R. E. DeMicheli, and R. S. Porter, *J. Polym. Sci., Polym. Lett.*, **21**, 791 (1983).
14. S. Kojima and R. S. Porter, *J. Polym. Sci., Polym. Phys. Ed.*, **16**, 1729 (1978).
15. G. Capaccio, T. A. Crompton, and I. M. Ward, *J. Polym. Sci., Polym. Phys. Ed.*, **14**, 1641 (1976).
16. H. Ashizawa, J. E. Spruiell, and J. D. White, *Polym. Eng. Sci.*, **24**, 1035 (1984).

Received November 13, 1984

Accepted February 12, 1985